

## IMPROVED SATELLITE-BASED VOLCANIC ASH DETECTION AND HEIGHT ESTIMATES

Michael J. Pavolonis\*

NOAA/NESDIS – Office of Research and Applications – Madison, WI

Wayne F. Feltz

Cooperative Institute for Meteorological Satellite Studies  
University of Wisconsin – Madison, WI

Andrew K. Heidinger

NOAA/NESDIS – Office of Research and Applications – Madison, WI

### 1. INTRODUCTION

Volcanic aerosols pose a serious danger to aircraft. In the past 30 years, more than 105 encounters of aircraft with airborne volcanic ash have been documented, with 25% of those encounters resulting in significant damage and/or engine failure (Miller and Casadevall, 2000). Fortunately, there have been no fatalities, but the financial impact of such encounters has been incredible. For instance, damage in the past 15 years has been estimated at more than \$250M. Many of these encounters could have been prevented with more advanced use of satellite data to detect and monitor volcanic aerosols.

Current operational volcanic ash detection techniques used at the Volcanic Ash Advisory Centers (VAAC's) are typically qualitative and require manual analysis. These qualitative techniques typically rely on a variety of satellite-based imaging instruments such as the Moderate Resolution Imaging Spectroradiometer (MODIS), the Advanced Very High Resolution Radiometer (AVHRR), and various geostationary imagers. Regardless of the instrument, a complete reliance on qualitative techniques presents some problems. For instance, even significant eruptions may not be identified in a timely manner using qualitative techniques, if the eruption is unexpected and the volcano is unmonitored (e.g. The May 10, 2003 eruption of Anatahan). Current operational techniques are also not particularly sensitive to volcanic aerosol clouds that are mixed with cloud water. In summary, auto-generated volcanic aerosol detection products should not be a substitute for qualitative techniques used by trained analysts, but should be used as a complementary information source that can help increase the

timeliness and accuracy of volcanic aerosol advisories.

Once a volcanic cloud has been detected in the horizontal, it is then imperative to determine if the volcanic cloud is located at aircraft cruising altitudes. The vertical location of volcanic clouds also influences dispersion, hence accurate forecasts of the location of ash are highly dependant on the height. At the present, operational estimates of volcanic cloud height are often limited to surface observations, inaccurate infrared window-based satellite methods, and wind correlation techniques. The purpose of this paper is to highlight some new automated satellite-based techniques for detecting volcanic aerosols (mainly volcanic ash) and determining the height of volcanic clouds that will improve upon current operational capabilities.

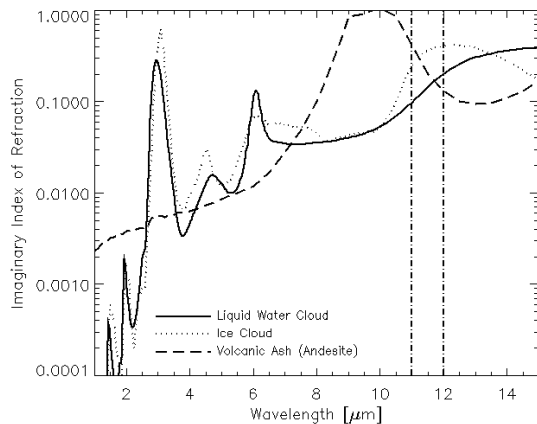
### 2. SPECTRAL SIGNATURE OF VOLCANIC CLOUDS

Figure 1 below shows the imaginary index of refraction of volcanic ash (modeled as andesite mineral) (Pollack et al., 1973), liquid water (from Downing and Williams, 1975), and ice (from Warren, 1984 and Gosse et al., 1995) as a function of wavelength. The imaginary index of refraction is directly proportional to absorption/emission strength for a given species composition and particle distribution, in that larger values are indicative of stronger absorption of radiation at a particular wavelength. From Figure 1, it is clear that ash will absorb more strongly at 11  $\mu\text{m}$  than at 12  $\mu\text{m}$ , while the opposite is true for water and ice clouds. Thus, liquid water clouds, ice clouds, and clear sky are generally characterized by positive 11  $\mu\text{m}$  minus 12  $\mu\text{m}$  brightness temperature differences (hereafter  $\text{BTD}[11,12]$ ), while a "pure" non-opaque volcanic ash cloud in a dry atmosphere will have a negative  $\text{BTD}[11,12]$ . This property is the basis of the reverse absorption technique (e.g. Prata, 1989a, 1989b), which in part seeks to identify negative  $\text{BTD}[11,12]$  values. Unfortunately, the reverse

---

\* *Corresponding author address:* Michael J. Pavolonis, NOAA/NESDIS/ORA, 1225 West Dayton Street, Madison, WI, 53706; e-mail: Mike.Pavolonis@noaa.gov.

absorption technique has limitations that have been well documented and understood (e.g. Prata et al., 2001). The main limitation is that many volcanic clouds reside in moisture rich environments which act to mask the negative BTD[11,12] volcanic cloud signal. The goal of our volcanic cloud detection work is to supplement the reverse absorption technique with additional spectral tests in order to improve detection sensitivity while reducing false alarms on a global basis.



**Figure 1:** The imaginary index of refraction of liquid water (solid), ice (dotted), and volcanic ash (andesite) (dashed) as a function of wavelength. The dash-dot lines intersect the three curves at 11 and 12  $\mu\text{m}$ .

The single scatter albedo (ssa) of volcanic ash (spherical andesite) for 3 different lognormal size distributions are shown in Figure 2 as a function of wavelength. The ssa for a large range of spherical liquid water droplets and non-spherical ice crystals (Nasiri et al., 2002) are also shown at the 0.65  $\mu\text{m}$  and 3.75  $\mu\text{m}$  wavelengths in Figure 2. The ssa can be interpreted as the probability that a photon will be scattered, given an extinction event. Note that, analogously ( $1.0 - \text{ssa}$ ) can be interpreted as the probability of a photon being absorbed, given an extinction event. Using the information in Figure 2 as a reference, and assuming that the ssa is a fair predictor of the relative magnitude of the satellite-measured reflectance, and using the information in Figure 1, the following properties can be used as the physical basis to develop a new automated volcanic cloud detection technique. This list is only a brief summary, a full discussion can be found in Pavolonis et al., 2005b. For a single layer liquid water cloud, ice cloud, and volcanic cloud of the same optical depth the following properties can be inferred. (1). The 0.65  $\mu\text{m}$  reflectance ( $R[0.65]$ ) of liquid water and ice clouds will tend to be greater than the  $R[0.65]$  for volcanic clouds. (2). Water and volcanic clouds will often have similar reflectance values at 3.75  $\mu\text{m}$  ( $R[3.75]$ ), while both tend to be

more reflective than ice clouds. (3). Thus, the ratio of  $R[3.75]/R[0.65]$  ( $RAT[3.75,0.65]$ ) for volcanic clouds will often be larger than  $RAT[3.75,0.65]$  for water and ice clouds. (4). Very cold clouds ( $BT[11] < 233 \text{ K}$ ) with a  $REF[3.75]$  that is typical of a water cloud, are likely heavily contaminated with aerosols, consistent with a volcanic eruption.

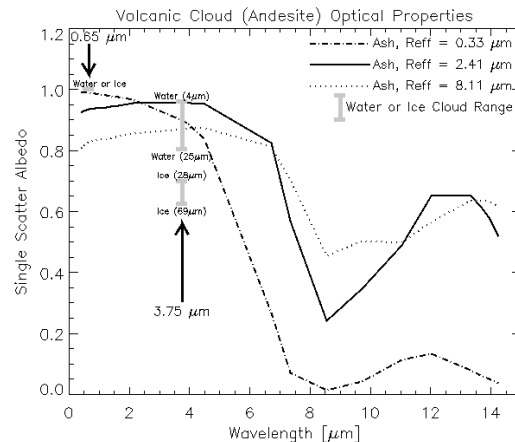


**Figure 2:** The single scatter albedo as a function of wavelength for three lognormal size distributions of volcanic ash. A typical range in single scatter albedo for liquid water and ice clouds is also overlaid at 0.65 and 3.75  $\mu\text{m}$ .

### 3. DAYTIME VOLCANIC ASH DETECTION

Based on the properties described in Section 2, an automated volcanic cloud detection algorithm that utilizes four spectral channels (0.65  $\mu\text{m}$ , 3.75  $\mu\text{m}$ , 11  $\mu\text{m}$ , and 12  $\mu\text{m}$ ) that are available on several satellite-based instruments was developed for daytime scenes. This new algorithm is physically based and globally applicable and can provide quick information on the horizontal location of volcanic clouds that can be used to improve real-time ash hazard assessments. This algorithm is described in great detail in Pavolonis et al. (2005b), so only an example is shown here.

The four channel daytime algorithm was applied to *Aqua* MODIS data that captured an eruption of Manam, PNG on October 24, 2004 (0355 UTC). This eruption occurred in a very moist and cloudy environment. Figure 3 shows three true color MODIS images of the Manam scene. The volcanic ash dominated cloud appears brown. In the bottom left panel, the results of the new 4-channel volcanic cloud algorithm are overlaid, and on the bottom right panel pixels with a  $BTD[11,12] < 0.0 \text{ K}$  are highlighted. The top right panel shows a colorized 11  $\mu\text{m} - 12 \mu\text{m}$  brightness temperature image. The four-channel algorithm produces a mask with two volcanic cloud categories, ash-dominated and ice clouds that may be contaminated with volcanic aerosol. The standard

reverse absorption algorithm (bottom right panel) is only able to detect a small portion of the core of the volcanic cloud, while the four-channel algorithm is able to successfully identify nearly all of the volcanic cloud that is not totally obscured by overlying cirrus cloud. The new algorithm also flags a large region next to the main ash cloud as being an ice cloud that is contaminated with volcanic aerosol. This result cannot be verified by simply analyzing the true color image, so independent Atmospheric Infrared Sounder (AIRS) data were consulted. AIRS is a high spectral resolution grating spectrometer with thousands of channels in the 3.7  $\mu\text{m}$  – 15.4  $\mu\text{m}$  range. The AIRS is also located on the *Aqua* platform. AIRS SO<sub>2</sub> (SO<sub>2</sub> is often released in large quantities during volcanic eruptions) imagery obtained from <http://toms.umbc.edu> (not shown) indicates that this ice cloud region is characterized by a very large SO<sub>2</sub> signal. This cloud may or may not contain silicate ash, but nevertheless is a hazard to aviation in and of itself due to the corrosive nature of high SO<sub>2</sub> concentration clouds. Thus, identifying such a cloud is useful. Finally, the reverse absorption technique produces scattered false alarms associated with convective clouds while the four-channel algorithm produces no noticeable false alarms.

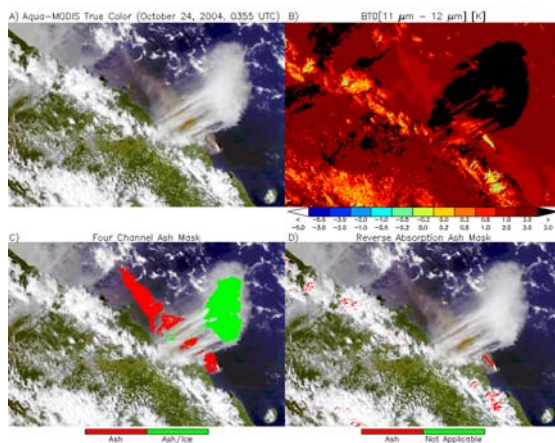


**Figure 3:** A four panel image showing an *Aqua* MODIS scene with a volcanic cloud produced from an eruption of Manam, PNG. The image is from October 24, 2004 at 03:55 UTC. A). a 1-km true color image created using the 0.65  $\mu\text{m}$ , 0.56  $\mu\text{m}$ , and 0.47  $\mu\text{m}$  channels B). a color-enhanced 11  $\mu\text{m}$  – 12  $\mu\text{m}$  brightness temperature difference image C). the same as Panel A, except the results of the four channel volcanic cloud detection algorithm are overlaid D). the same as Panel A, except the results of the reverse absorption detection algorithm are overlaid.

#### 4. NIGHTTIME VOLCANIC ASH DETECTION

With no reflective channel data available, detection of volcanic ash at night is much more challenging. Current efforts have focused on using a tri-spectral approach with the 3.75  $\mu\text{m}$ , 11  $\mu\text{m}$ , and 12  $\mu\text{m}$  channels, since these channels are available on most satellite imaging instruments. This sort of approach was discussed in Ellrod et al. (2003) for qualitative volcanic cloud detection. The nighttime algorithm operates under the premise that volcanic clouds will tend to have small (positive) or negative BTD[11,12] values, typical of opaque meteorological clouds, and relatively large 3.75  $\mu\text{m}$  minus 11  $\mu\text{m}$  brightness temperature differences, which are typical of semi-transparent ice clouds, creating a set of observations not normally associated with meteorological clouds. The nighttime algorithm is still under development so these are only preliminary results. Figure 4 shows the results of the nighttime volcanic cloud mask using NOAA-17 AVHRR data for the March 09, 2005 minor eruption of Mount St. Helens, Washington. Even though the accompanying imagery indicates that this volcanic cloud is very optically thin, the algorithm is able to detect most of the cloud, while producing little or no false alarms even though several non-volcanic cloud pixels have a negative BTD[11,12] (not shown)]. Much more work remains to be done on the nighttime volcanic cloud detection algorithm. On sensors such as MODIS, spectral channels in the 6.7  $\mu\text{m}$ , 7.4  $\mu\text{m}$ , and 8.5  $\mu\text{m}$  regions should offer enhanced nighttime detection capabilities.

#### 5. VOLCANIC CLOUD HEIGHT DETERMINATION

Identifying the height of a volcanic cloud from satellite observations can be very difficult, particularly when it is semi-transparent. At operational VAAC's, height identification is frequently performed by observing plume drift and then consulting global model wind fields to find the height of a corresponding wind vector. When the atmosphere exhibits directional shear, this can be a very accurate approach, but it cannot be relied upon for all situations. Further, determining the height by matching the observed 11  $\mu\text{m}$  brightness temperature with the height corresponding to the same temperature in an atmospheric profile is very inaccurate when applied to semi-transparent clouds. Thus, more advanced satellite-based techniques are needed to determine the height of volcanic clouds. One such method is the CO<sub>2</sub> slicing technique (e.g. Wylie and Menzel, 1989), which utilizes infrared channels dominated by CO<sub>2</sub> absorption to iteratively determine cloud height. CO<sub>2</sub> slicing is especially sensitive to high altitude semi-transparent clouds. Much more information on the application of the CO<sub>2</sub> slicing technique to volcanic clouds is given in Paper 8.6 of these

proceedings. Unfortunately, many satellite imagers do not or will not have CO<sub>2</sub> absorption channels (e.g. AVHRR, MTSAT, Visible/Infrared Imager/Radiometer Suite (VIIRS)), so the development of another alternative method would be useful.

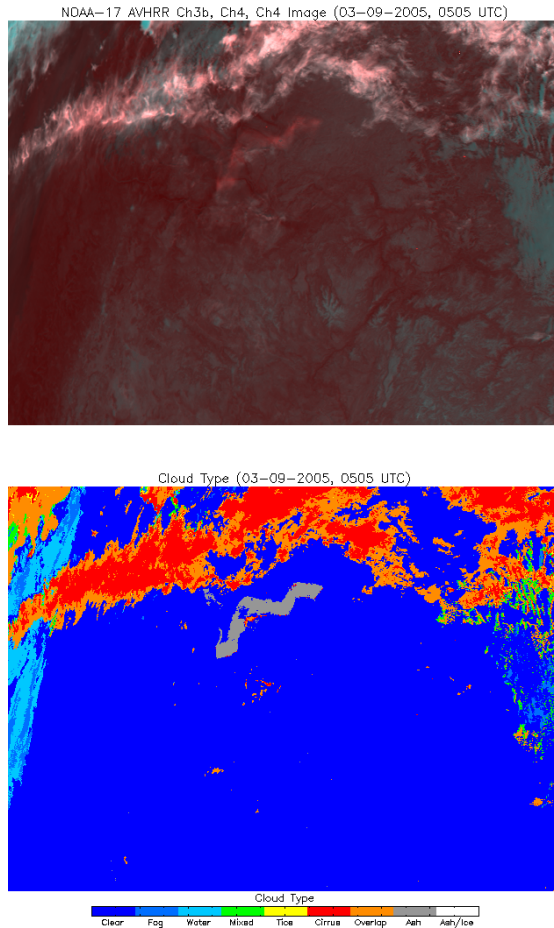


**Figure 4:** A two panel image showing a NOAA-17 AVHRR scene with a volcanic cloud produced from a small eruption of Mount St. Helens, WA. The image is from March 09, 2005 at 05:05 UTC. Shown on top is a 1-km two-channel (3.75  $\mu\text{m}$  and 11  $\mu\text{m}$ ) RGB image. Shown on bottom is the resulting pixel level cloud type produced from an automated algorithm. Volcanic ash is shown in gray.

Like CO<sub>2</sub> slicing, the new method presented here accounts for the often semi-transparent nature of clouds (volcanic or otherwise) and is called the “split window” method because it utilizes satellite measurements in the 11  $\mu\text{m}$  and 12  $\mu\text{m}$  channels. The split window algorithm simultaneously retrieves cloud top temperature and cloud emissivity using an optimal estimation approach (e.g. Marks and Rodgers, 1993). The split window technique operates under the premise that for a known atmospheric state, surface

temperature, and surface emissivity, the 11  $\mu\text{m}$  and 12  $\mu\text{m}$  measurements for a single layer cloud are primarily determined by three factors: (1) cloud temperature, (2) cloud emissivity, and (3) cloud particle size and shape distribution. Further, the radiative effect of the particle size and shape distribution is captured in the quantity,  $\beta$  (Parol et al., 1991), a ratio of the 12  $\mu\text{m}$  and 11  $\mu\text{m}$  cloud emissivities. If the cloud type (volcanic clouds included) of an individual pixel is determined, a reasonable assumption about the particle size and shape characteristics can be made, leaving only the cloud temperature and 11  $\mu\text{m}$  emissivity to be retrieved within the optimal estimation (1D-VAR) system from the measured 11  $\mu\text{m}$  and 12  $\mu\text{m}$  radiances. The resultant cloud temperature can then be matched to a pressure and/or height within an atmospheric sounding as is performed within the CO<sub>2</sub> slicing technique. In order to determine cloud type the techniques of Pavolonis and Heidinger (2004), Pavolonis et al. (2005a), Pavolonis and Heidinger (2005), and Pavolonis et al. (2005b) are used to classify cloudy satellite pixels as having fog, liquid water cloud (fog not included), supercooled water cloud, opaque ice cloud, cirrus cloud, multilayered cloud, volcanic ash, and volcanic ash/ice. The cloud type is also used to determine the first guess estimate of the cloud top temperature and emissivity in the optimal estimation retrieval scheme. The split window algorithm is described in much more detail in Heidinger and Pavolonis (2005b) and also summarized in Heidinger et al. (2005a).

Figure 5 shows the results of the split window cloud height and emissivity retrieval for the October 24, 2004 eruption of Manam, PNG. This is the same scene shown in Section 3. As can be seen, the height of the elongated ash-dominated volcanic cloud, which appears brown in the true color image (also refer to the volcanic cloud mask shown in Figure 3), decreases in height and emissivity going away from the volcano. This behavior is expected since ash fallout will occur away from strong updrafts. Using wind correlation and other methods the Darwin VAAC estimated this same volcanic cloud to be at a height of about 5000 – 6000 m, which is consistent with the split window retrieved heights. The heights and emissivity within the volcanic aerosol - contaminated ice cloud (again see Figure 3) indicate that this cloud was located in the upper troposphere and is rather optically thick.

Future work will focus on “validating” the split window heights against CO<sub>2</sub> slicing derived heights and other independent methods using passive and active remote sensing instruments.

## 6. CONCLUSION

This paper summaries some improved techniques for detecting volcanic clouds and

determining their vertical location. The algorithms are computationally efficient, so operational implementation is very feasible. These techniques can be applied to a variety of sensors such as GOES, MTSAT, and AVHRR. Further, current instruments like the MODIS and the Spinning Enhanced Visible and Infrared Imager (SEVIRI) offer an even better opportunity to detect volcanic clouds, especially at night, and future sensors such as the Advanced Baseline Imager (ABI) on the GOES-R platform (~2013 launch) and the Visible/Infrared Imager/Radiometer Suite (VIIRS) on the National Polar-orbiting Operational Environmental Satellite System (NPOESS) (~2008 launch) will also offer additional operational capabilities. Future work will focus on utilizing these additional capabilities for volcanic cloud detection and property retrievals. It is also possible that in the future the best approach to generating an automated volcanic aerosol mask and retrieving volcanic cloud properties will be to combine information from narrow band imagers and hyperspectral infrared sounders. The hyperspectral sounder may provide a means to better detect sub-visible volcanic clouds and/or volcanic clouds composed of mainly SO<sub>2</sub> and H<sub>2</sub>SO<sub>4</sub>. The MODIS/AIRS combination can be used to develop these algorithms in preparation for these future satellite missions.

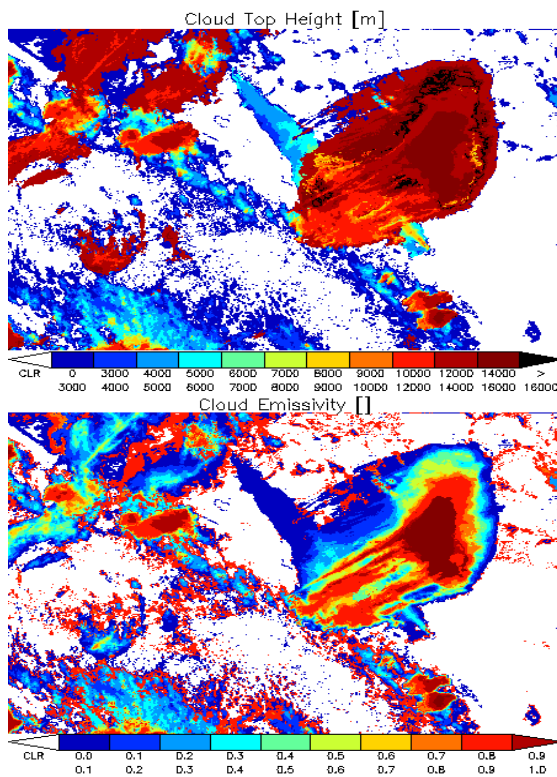


**Figure 5:** The results of the split window cloud top height (top) and emissivity (bottom) retrieval for the Manam scene first shown in Figure 3.

## 7. ACKNOWLEDGEMENTS

This work was supported by the NASA Applied Science Program and the NASA Aviation Safety and Security Program through the NASA Advanced Satellite Aviation-weather Products (ASAP) project. The views, opinions, and findings contained in this paper are those of the authors and should not be construed as an official National Oceanic and Atmospheric Administration or U.S. Government position, policy, or decision.

## 8. REFERENCES

Downing, H. D., and D. Williams, 1975: Optical constants of water in the infrared. *J. Geophys. Res.*, **80**, 1656-1661.

Ellrod, G. P., B. H. Connell, and D. W. Hillger, 2003: Improved detection of airborne volcanic ash using multispectral infrared satellite data. *J. Geophys. Res.*, **108**, 4356.

Gosse, S., D. Labrie, and P. Chylek, 1995: Refractive index of ice in the 1.4-7.8  $\mu\text{m}$  spectral range. *Appl. Opt.*, **34**, 6582-6586.

Heidinger, A. K., M. D. Goldberg, D. Tarpley, A. J. Jelenak, and M. J. Pavolonis, 2005a: A new AVHRR cloud climatology. International Asia-Pacific Environmental Remote Sensing Symposium, 4th: Remote Sensing of the Atmosphere, Ocean, Environment, and Space, Honolulu, Hawaii, 8-11 November 2004. Applications with Weather Satellites II (proceedings). Bellingham, WA, International Society for Optical Engineering, (SPIE), 197-205.

Heidinger, A. K. and M. J. Pavolonis, 2005b: A multi-year global climatology of cloud temperature and emissivity from the AVHRR split-window observations. Part I: Approach and expected accuracy. In prep.

Marks, C. J., and C. D. Rodgers, 1993: A retrieval method for atmospheric composition from limb emission measurements. *J. Geophys. Res.*, **98**, 14 939 – 14 952.

Miller, T. P., and T. J. Casadevall, 2000: Volcanic ash hazards to aviation. *Encyclopedia of Volcanoes*, edited by H. Sigurdsson, pp. 915-930, Academic, San Diego, CA.

Nasiri, S. L., B. A. Baum, A. J. Heymsfield, P. Yang, M. R. Poellot, D. P. Kratz, and Y. X. Hu, 2002: The development of midlatitude cirrus models for MODIS using FIRE-I, FIRE-II, and ARM in situ data. *J. Appl. Meteor.*, **41**, 197-217.

Parol, F., J. C. Buriez, G. Brogniez, U. Fouquart, 1991: Information content of AVHRR Channels 4 and 5 with respect to effect radius of cirrus cloud particles. *J. Appl. Meteor.*, **30**, 973-984.

Pavolonis, M. J. and A. K. Heidinger, 2004: Daytime cloud overlap detection from AVHRR and VIIRS. *J. Appl. Meteorol.*, **43**, 762-778.

Pavolonis, M. J., A. K. Heidinger, and T. Uttal, 2005a: Daytime global cloud typing from AVHRR and VIIRS: Algorithm description, validation, and comparisons. *J. Appl. Meteorol.*, **44**, 804-826.

Pavolonis, M. J., W. F. Feltz, A. K. Heidinger, and G. M. Gallina, 2005b: A daytime complement to the reverse absorption technique for improved automated detection of volcanic ash. Submitted to *J. Atmos. and Oceanic Tech.*

Pavolonis, M. J. and A. K. Heidinger, 2005: Advancements in identifying cirrus and multilayered cloud systems from operational satellite imagers at night. International Asia-Pacific Environmental Remote Sensing Symposium, 4th: Remote Sensing of the Atmosphere, Ocean, Environment, and Space, Honolulu, Hawaii, 8-11 November 2004. Applications with Weather Satellites II (proceedings). International Society for Optical Engineering, (SPIE), Bellingham, WA, 2005, pp.225-234.

Pollack, J. B., O. B. Toon, and B. N. Khare, 1973: Optical properties of some terrestrial rocks and glasses. *Icarus*, **19**, 372-389.

Prata, A. J., 1989a: Observations of volcanic ash clouds in the 10 –12 micrometer window using AVHRR/2 data. *Int. J. Rem. Sen.*, **10**, 751-761.

Prata, A. J., 1989b: Radiative transfer calculations for volcanic ash clouds. *Geophysical Res. Letters*, **16 (11)**, 1293-1296.

Prate, A. J., G. Bluth, B. Rose, D. Schneider, and A. Tupper, 2001: Failures in detecting volcanic ash from a satellite-based technique – Comments. *Remote Sens. Environ.*, **78**, 341-346.

Warren, S., 1984: Optical constants of ice from the ultraviolet to the microwave. *Appl. Opt.*, **23**, 1206-1225.

Wylie, D. P., and W. P. Menzel, 1989: Two years of cloud cover statistics using VAS. *J. Climate*, **2 (4)**, 380-392.